DEUTSCHES ELEKTRONEN-SYNCHROTRON DESY

DESY 69/12
March 1969



# Secondary Electron Emission of Metal Foils in the Energy Range of 1.5-7 GeV

by

E. Raquet

2 HAMBURG 52 · NOTKESTIEG 1

# Secondary Electron Emission of Metal Foils in the Energy Range of 1.5 - 7 GeV

by

E. Raquet

Abstract

The secondary emission properties of single metal foils have been investigated for the purpose of designing a secondary emission monitor with a minimum scattering length. The first part of this report deals with the more basic behaviour of the secondary emission. For an understanding of the emission from thin metal foils two results seem to be important:

a. The ratio of the secondary emission from the beam entrance surface of the foil to that from the beam exit surface is roughly 2:1.

b. In agreement with a theoretical treatment by Aggson, the emission from the entrance surface depends on the primary energy, while the emission from the exit surface is independent.

In the second part some applications are briefly described.

## I. Introduction

Low energy secondary electrons (SE) are emitted when a high energy beam of charged particles traverses a thin metal foil. The secondary emission coefficient of the usual metals is only a few percent. Therefore the most commonly secondary emission monitors[1,2] consist of a set of 10 to 20 foils to obtain a SE current comparable to the primary current.

On the other hand, in many cases one wishes to minimize the scattering length of the monitor in order to avoid a deterioration of the beam. This problem becomes serious, for instance, when two different experiments are arranged on the same beam, or when the beam intensity has to be measured upstream the target for the beam adjustment. In both cases a monitor is required consisting of a single foil only and operating inside the beam transport vacuum. The mechanical structure of the monitor should be as simple as possible with small dimensions for the use of motion of the monitor into or out of the beam.

Because of their low energies (< 100 eV) the maximum depth that the SE are able to escape, is about 100 Å.[3] Thus the surface conditions of the foils play a dominant role for the SE emission.

Using aluminum foils the vacuum of the monitor must be maintained at least at $10^{-7}$ torr because of the sensitivity of the foil surfaces. This requires a separation between the rougher beam transport vacuum and the monitor vacuum. The total scattering length of the monitor is thus enlarged by its windows. The coating by vacuum evaporation of aluminum foils with very thin gold layers (0.1 micron) is difficult and does not give homogeneous surfaces with constant surface properties at a lower vacuum.[4]

Pure noble metal foils, e.g. gold, exhibit more constant surface properties even in a lower vacuum. The thinnest available foils of some microns thickness have radiation lengths of $10^{-3}$ - $10^{-4}$ and fulfill the required conditions.

The measuring of the emission current from a single foil is not difficult with the beam intensities and integrators available at present. For very low beam intensities a quite different method for detecting SE is described below.

In order to investigate the emission qualities of a single foil, various measurements were made with a 10 microns gold foil and 4 aluminum foils of 8, 25, 50, and 100 microns in thickness. The first part of the measurements deals with the more basic properties of the secondary emission from a single foil. In the second part some applications are briefly described.

## II. Secondary Emission from a Single Foil

### 1. Measuring Device

Fig.1 shows a schematic diagram of the measuring device. The SE escaping from both sides of the foil are either accelerated from the surface or retained on the surface, depending on the potentials of the grids in front of each foil side. The grids have a high transparency of about 98%. The distance between grids and foil is 10 mm, the diameter of both 180 mm. The emission current of the foil is measured by an integrator. Both grids are galvanically separated for independent variation of the grid potentials. Thus a discrimination is possible between the SE escaping from the upstream surface ($\overleftarrow{SE}$) and the SE escaping from the downstream surface ($\overrightarrow{SE}$). The vacuum of the monitor chamber was maintained at $10^{-5}$ - $10^{-6}$ torr.

### 2. Secondary Emission Differences between the Upstream and Downstream Surfaces of the Foil

Fig.2 shows, as a typical example, the dependence of the emission current of the 25 microns aluminum foil on various grid potentials. The primary energy was 3.3 GeV. Curve 1 has been obtained by varying the potentials of both grids simultaneously, Curve 2 by varying the potential of the upstream grid with the downstream grid potential kept constant (+200 V), and Curve 3 by varying the potential of the downstream grid with constant upstream potential. The distance SE in Fig.2 thus corresponds to the "true" SE with energies below about 100 eV. The distance $\overleftarrow{SE}$ corresponds to the "true" SE escaping from upstream foil surface, and the distance $\overrightarrow{SE}$ in Fig.2 corresponds to the "true" SE from the downstream surface. The portion of emitted electrons with medium energies above 100 eV (so-called $\delta$-electrons) amounts to 4.5% of the total emission.

For the result to be independent of differences between foil surface conditions and of the special arrangement, two conditions must be fulfilled.

a. It must be possible to rotate the monitor around its vertical axis by 180° without affecting the results.

b. The following equation must be valid

$$SE = \overleftarrow{SE} + \overrightarrow{SE}$$

This is not trivial because a mutual influence of the grid potentials could be possible due to edge effects.

Within the measuring accuracy of ±3% both requirements have been satisfied for each foil.

Expressed in percent of the total SE-current we found, independent of the investigated foil thickness, the somewhat surprising result:

$$SE(100\%) = \overleftarrow{SE}([66 \pm 3]\%) + \overrightarrow{SE}([34 \pm 3]\%) \qquad (1)$$

3. <u>Dependence of the Secondary Emission on the Primary Energy</u>

An investigation of the energy dependence of the secondary emission by the above method is very interesting with respect to the results of a theoretical treatment by Aggson.[4] According to Aggson the SE emission from the entrance surface should be dependent on the primary energy while the emission from the exit surface should be independent.

Since recent measurements at CEA and SLAC[5] have shown a relatively large effect of energy dependence for gold plated foils, we used a pure gold foil.

Fig.3 shows the results of our measurements.

a. The total emission of the foil increases by about 10% with increasing energy in the tested energy range of 1.5 - 7 GeV. The results are in good agreement with those of CEA and SLAC.

b. The total emission of "true" SE with energies below 100 eV also increases by 10%. This increase is due to the SE from the upstream foil surface only while the emission of the downstream foil surface remains constant within the measuring accuracy. This result agrees with Aggson's prediction.

c. Within the limits of Equation (1) the upstream secondary emission is about twice the downstream emission.

d. The emission of δ-electrons contribute about 22% to the total emission of the gold foil. By averaging data of various authors, S. P. Visvanathan et al.[6] gives the following relationship between δ-electron yield and foil thickness

$$R = 1.77 \times \ln(1 + 3t) \qquad (2)$$

R = δ-electron yield in percent of the primary beam
t = foil thickness [g $cm^{-2}$]

The first curve in Fig.4 represents Equation (2), including the data of Visvanathan and other authors. The data were obtained by counting the δ-electrons or by interpreting cloud chamber pictures. Our data for the four aluminum foils and the gold foil are also shown in Fig.4. The curve according to Equation (1) seems to decrease too steeply for small t-values. A fit including our data would give

$$R = \ln(1 + 100t) \qquad (3)$$

The efficiency of monitors consisting of a set of foils is increased by the δ-electrons. The SE yield for δ-electrons of medium energies is essentially higher than the yield for primary electrons.[7] Secondary emission coefficients obtained by averaging the total emissions of a foil set are therefore too large.

## III. Applications

### 1. Measurement of the Beam Intensity

If the monitor has the small dimensions and low radiation length mentioned in the introduction, the measuring device as shown in Fig.1 can be used directly. For this application the dependence of the foil response on the vacuum pressure is important. Fig.5 shows the decrease of the response of the gold foil within the first 20 minutes of the first irradiation at a relatively low vacuum of $5 \times 10^{-4}$ torr. From then on we obtained a reasonable constant response and in the cases of short break-downs up to 1 hour we did not observe a new decrease. Further investigations will be necessary for more detailed information. Nevertheless an improvement of the vacuum up to $10^{-5}$ torr seems to be sufficient for obtaining a reasonably good short time stability within the required accuracy of measuring runs over a few days.

## 2. Measurements of the Beam Profile

By subdividing the foil into a series of foil strips and by measuring the emission current of the strips consecutively, one obtains informations about the beam profile. Fig.6 shows the block diagram used, Fig.7 shows a photograph of the monitor, and Fig.8 two samples of beam profiles measured on our beam line 20 in front of the Faraday cup in Hall II a. The measuring sequence of the accumulated charge on each strip is about once per second. The voltages stored on the strips (which is proportional to the charges for equal capacities) go up to some hundred mV maximum for the usual beam intensities. The discharging of the strips occurs during the measuring procedure, but because of the fast rise-time of the amplifier as compared with the discharge time, the measuring error is negligiable. Nevertheless other circuits will be tested where the foil strip will be grounded for discharge after each measuring cycle.

## 3. Detection of the SE with an open SE Multiplier*

A drawback of all monitors measuring the SE current by integration is their low time resolution caused by the large time constant of the integration circuit. For example, the time resolution is not sufficient to get information about the intensity distribution over the spill time.

This disadvantage had been avoided and at the same time the linear response of the secondary emission as well as the high sensitivity and fast time resolution of SE multiplier tubes could be obtained by our references monitor device as shown in Fig.9. Fig.10 shows a picture of the device.

---

*A first description of this device was given at Symposium on Beam Intensity Measurement at Daresbury, 22 - 26 April 1968.

The SE emitted from the surface of the used aluminum foil are retarded or accelerated by an electrostatic field between the foil and a grid in front of the foil. In the case of acceleration the electrons pass through the grid and are focused onto the cathode of an open multiplier by one cylindrical electrode and two accelerating electrodes. The counting rate of the multiplier is therefore for small primary intensities proportional to the number of primary electrons.

Fig.11 shows the electrostatic field of the focusing electrodes measured in an electrolytic tank. Similar focusing assemblies were used in the case of photomultiplier tubes.[8]

Fig.12 represents the dependence of the counting rate per unit Faraday cup current on the focusing cylinder voltage. The voltage lies between the cylinder and the grid, which is 5 V positive with respect to the foil. Optimum focusing was obtained at +20 V cylinder voltage. From then on, the cylinder was fixed at this potential.

Fig.13 shows the effect of the electrostatic field between foil and grid. In case of an accelerating field, one gets a reasonable plateau. For a larger retarding field the counting rate decreases rapidly, because the secondary electrons have only low energies.

Fig.14 shows the range of the linear response against the primary intensity. Above the limit of about $5 \times 10^8$ electrons per machine pulse (1ms spilltime), the maximum pulse frequency of the multiplier (focused mesh type MM-1 by Johnston Laboratories, Inc.) exceeds the maximum counting rate of $10^8$ per second, even if the SE yield and the detection efficiency of the multiplier is reduced as far as possible. The threshold of the following discriminator has been chosen to suppress all pulses with amplitudes comparable to the multiplier noise pulses.

By again subdividing the foil into strips in the above manner, one can obtain information about the beam profile with a good time resolution. With the exception of one strip, a retarding potential is applied between the strips and the grid. Therefore only the SE from this strip can reach the multiplier. By changing to the next strip, e.g. within the time interval between machine spills, an information about the beam profile can be obtained. Preliminary measurements have been made but further development is necessary to achieve a well tested monitor with good reliability in operation.

Acknowledgement

I would like to thank Dr. D. Degèle for his kind interest he has shown in this work. The assistance of Messrs. D. Kessler, F. Peters, M. Rowold, and W. Stapelfeld in performing the measurements is gratefully acknowledged.

References

1. A. Ladage and H. Pingel, DESY Report 65/12 (1965)

2. J. dePagter and M. Fotino, CEAL-1022 (1965)

3. O. Hachenberg and W. Brauer, Advances in Electronics and Electron Physics, XI, 413, Academic Press (1959)

4. T. L. Aggson, Report L. A. L 1028, Orsay (1962)

5. G. F. Dell and M. Fotino, CEAL 1045 (1968)

6. S. P. Visvanathan et al., Nuovo Cimento 28, 850 (1963)

7. A. Ladage, DESY Report 65/16 (1965)

8. Valvo, Handbuch Spezialröhren II, (1967).

List of Figures

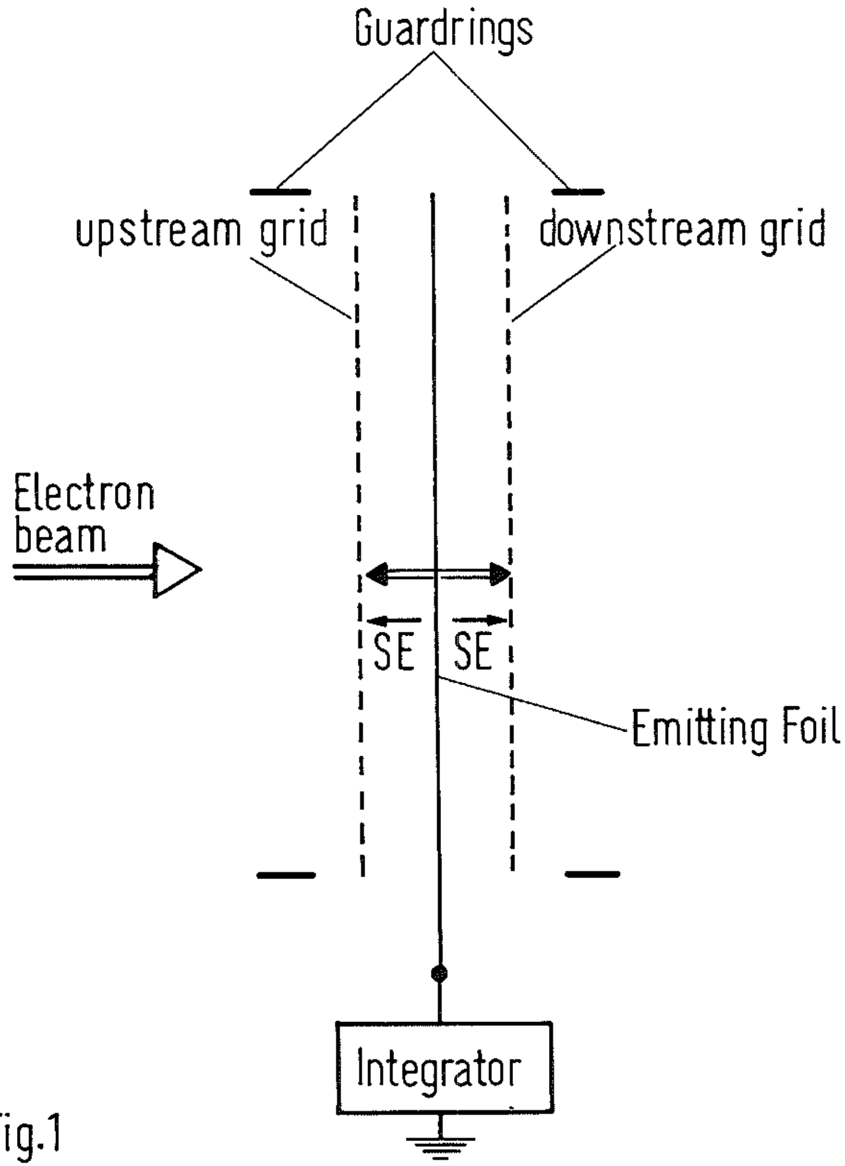


Fig.1
Schematic Diagram of the Measuring Device

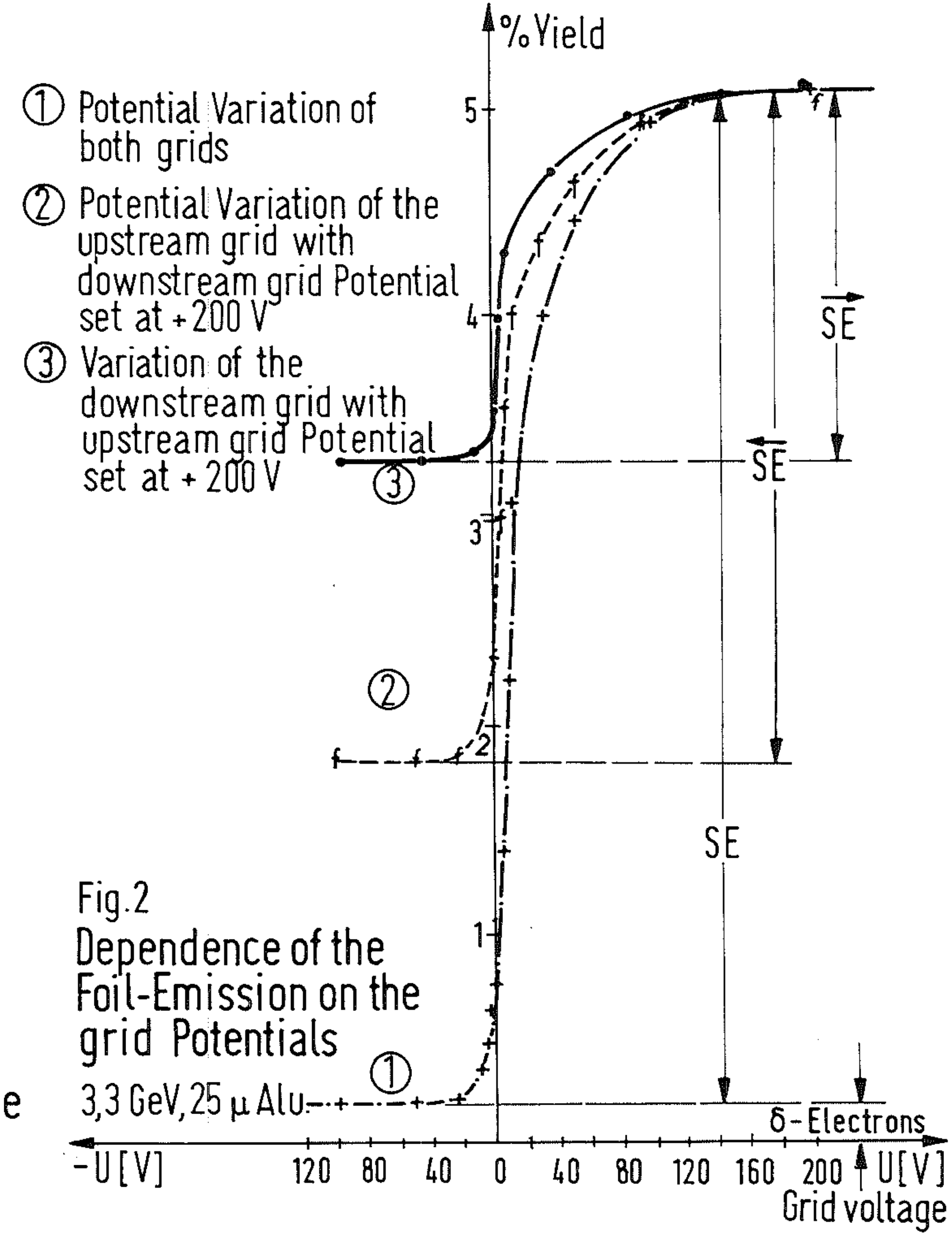


Fig.2
Dependence of the Foil-Emission on the grid Potentials
3,3 GeV, 25 µ Alu

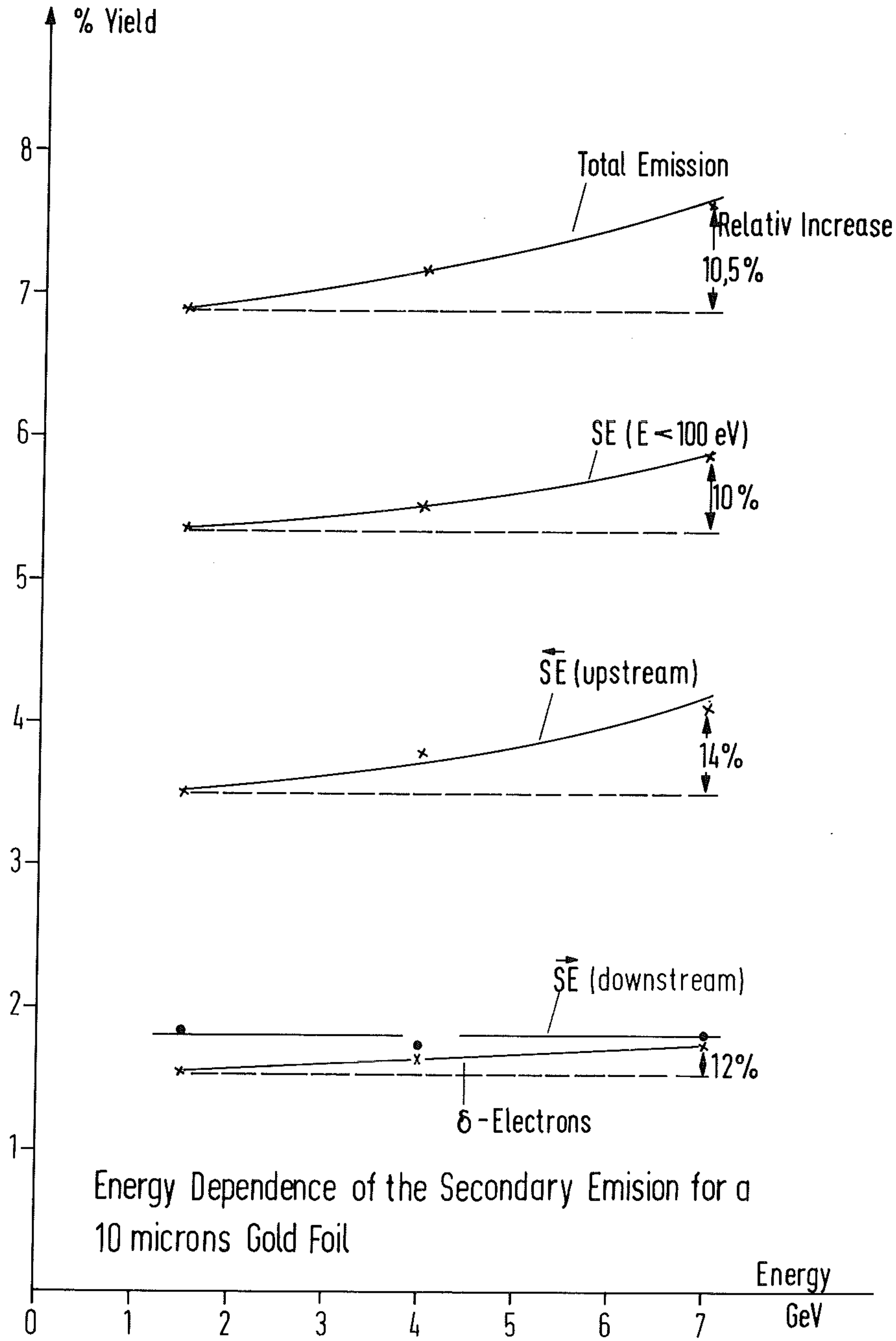
% Yield
8
7
6
5
4
3
2
1
Total Emission
Relativ Increase
10,5%
SE (E < 100 eV)
10%
SE (upstream)
14%
SE (downstream)
12%
δ-Electrons
Energy Dependence of the Secondary Emision for a
10 microns Gold Foil
Energy
GeV
0
1
2
3
4
5
6
7

Fig.3

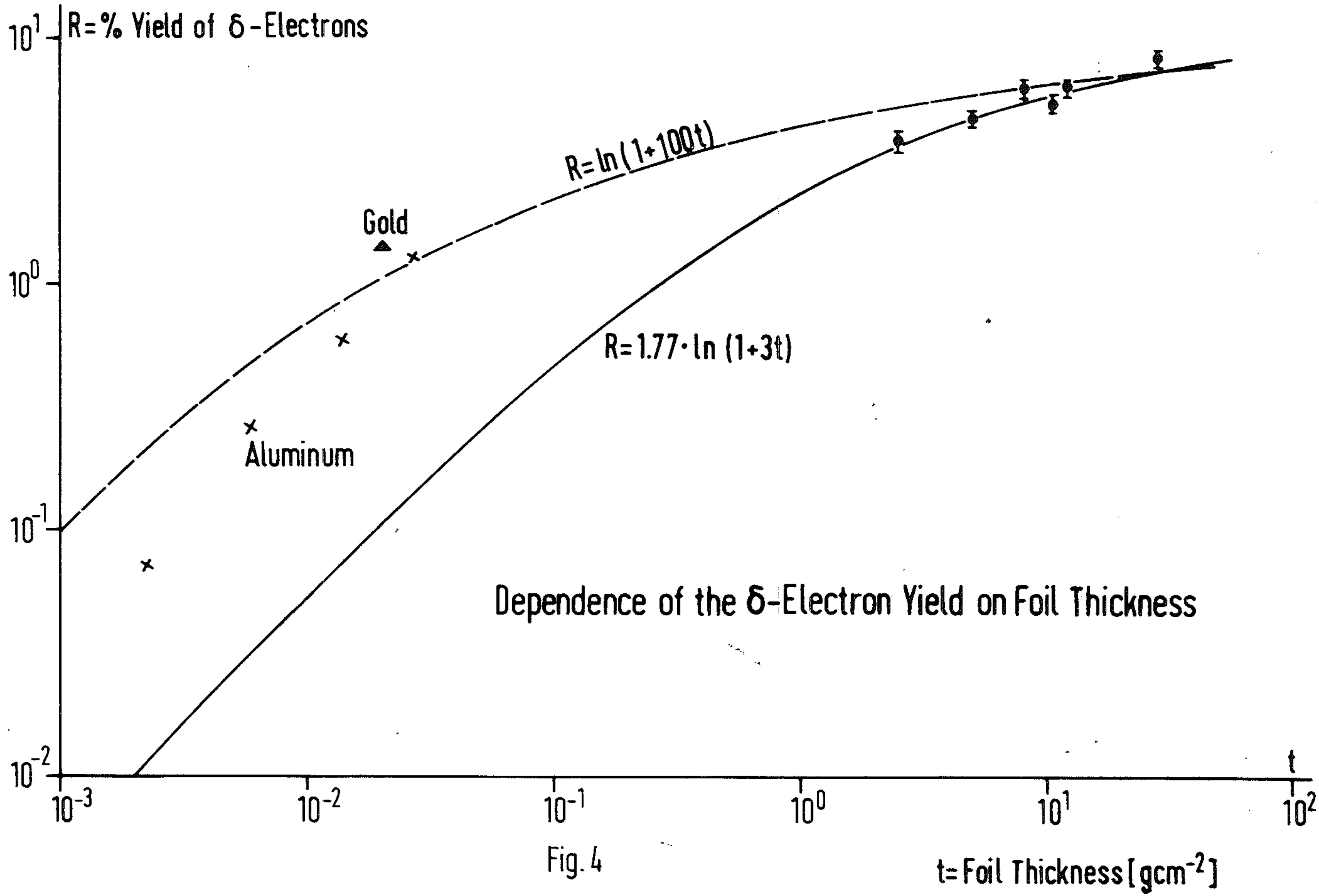
R = % Yield of δ-Electrons
$10^1$
$10^0$
$10^{-1}$
$10^{-2}$
R = ln (1+100t)
Gold
Aluminum
R = 1.77 · ln (1+3t)
Dependence of the δ-Electron Yield on Foil Thickness
t
$10^{-3}$
$10^{-2}$
$10^{-1}$
$10^0$
$10^1$
$10^2$
t = Foil Thickness [gcm$^{-2}$]

Fig. 4

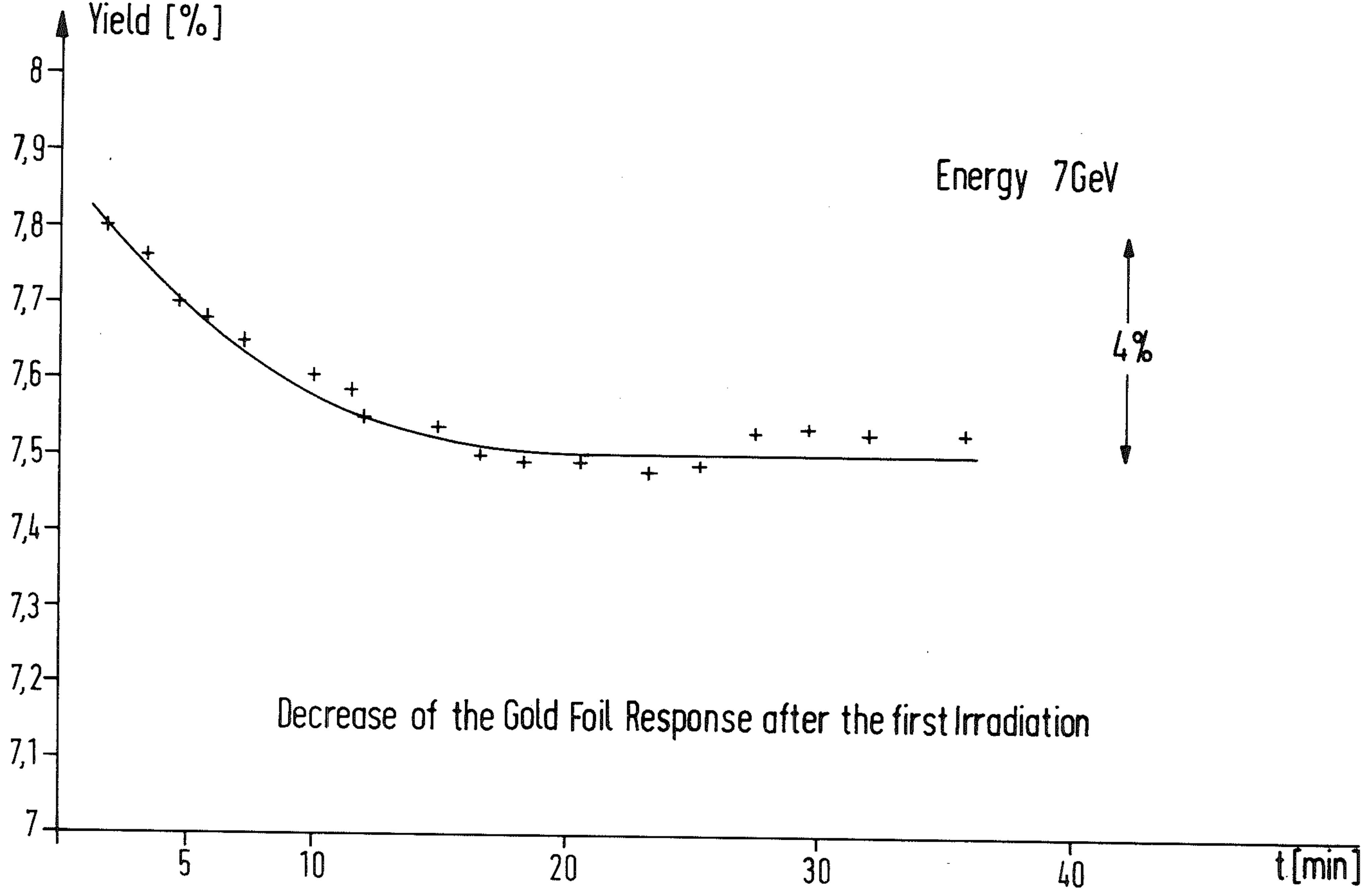
Yield [%]
8
7,9
7,8
7,7
7,6
7,5
7,4
7,3
7,2
7,1
7
5
10
20
30
40
t [min]
Energy 7GeV
4%
Decrease of the Gold Foil Response after the first Irradiation

Fig. 5

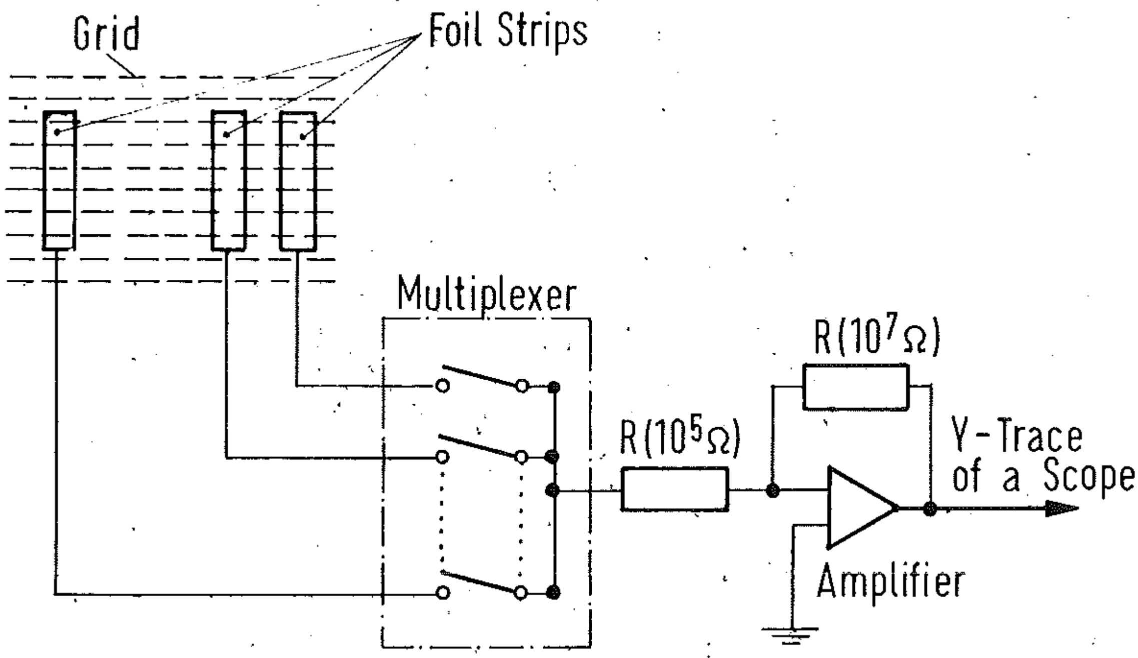


Fig.6 Block Diagram for the Foil Strips

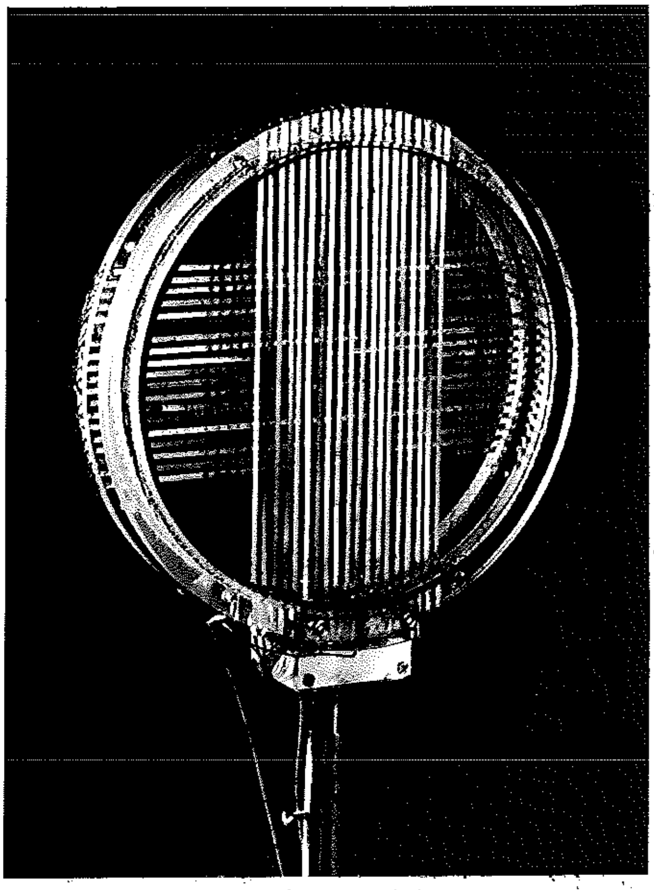

Fig.7 Monitor with crossed Foil Strips.
Strip Width = 2,5 mm
Strip Distance = 2,5 mm

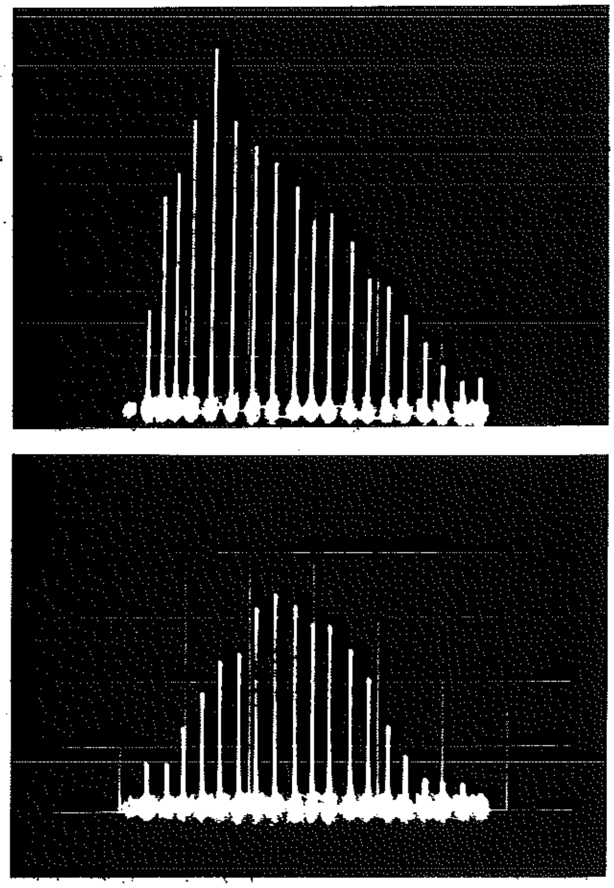

Fig.8 Two Samples of vertical Beam Profiles.
$E_0 = 3.3$ GeV
Beam Intensity $\approx 3 \cdot 10^{-8}$ A

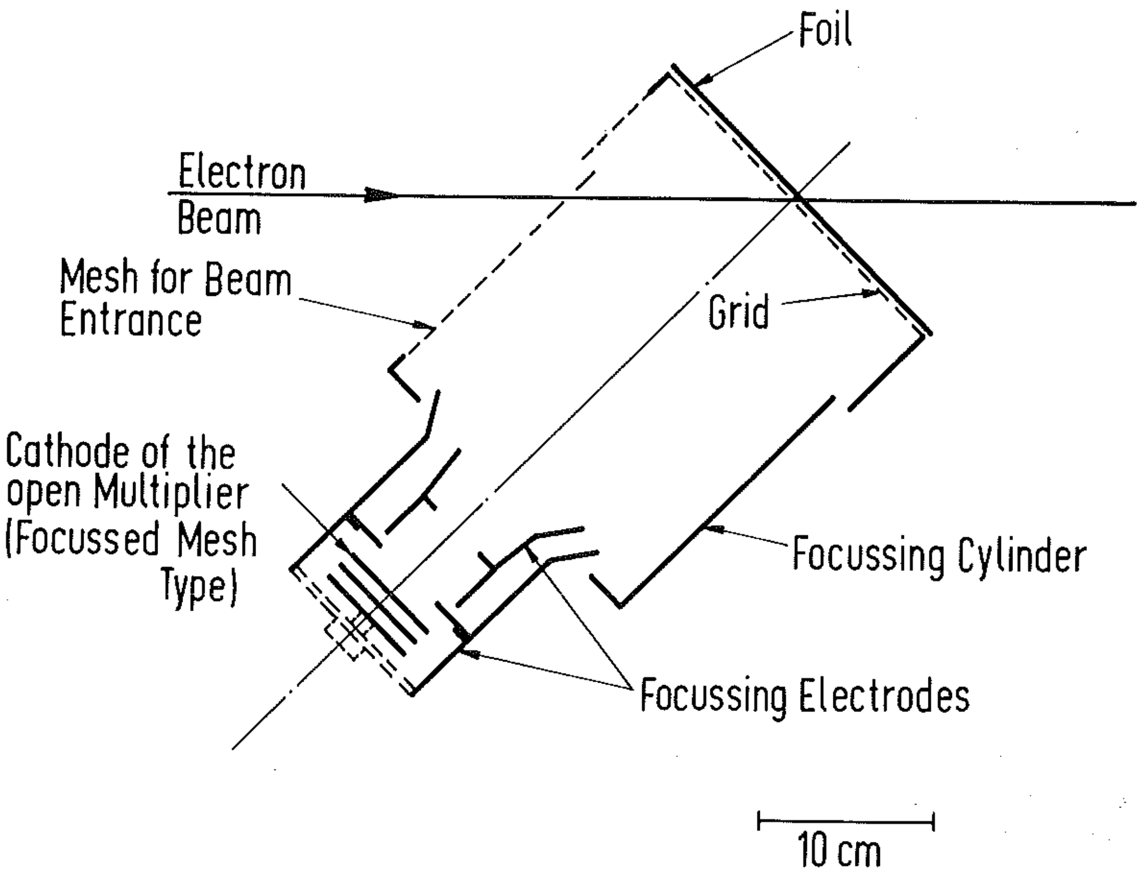


Fig.9 Schematic Diagram of the Monitor

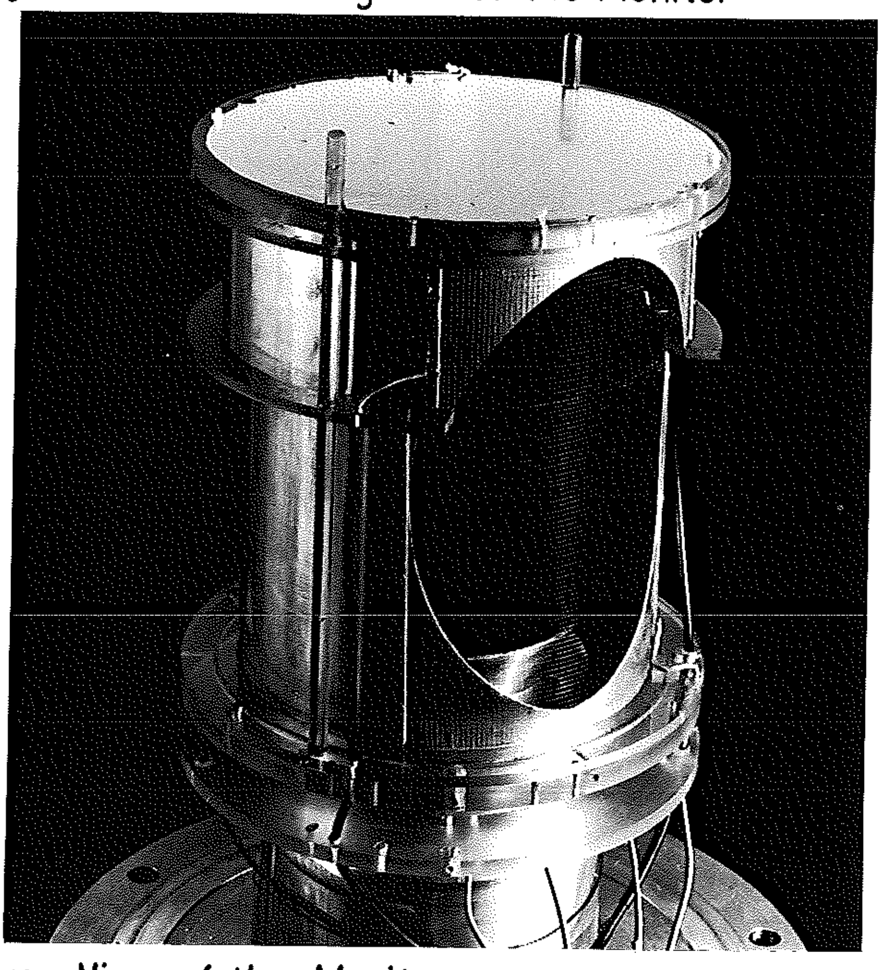

Fig.10 View of the Monitor

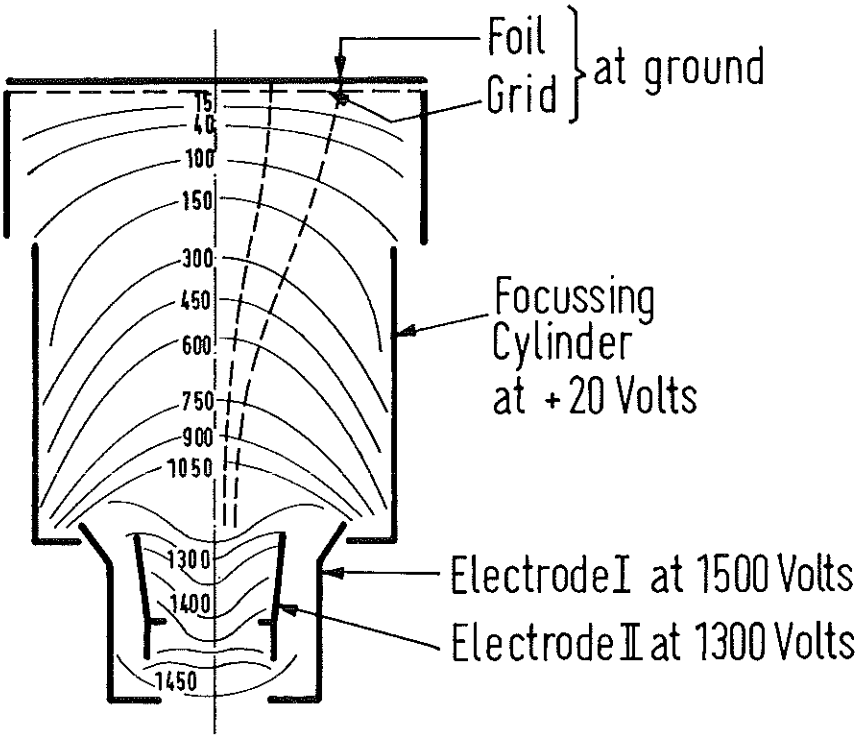


Fig.11 Focussing Field of the Electrodes

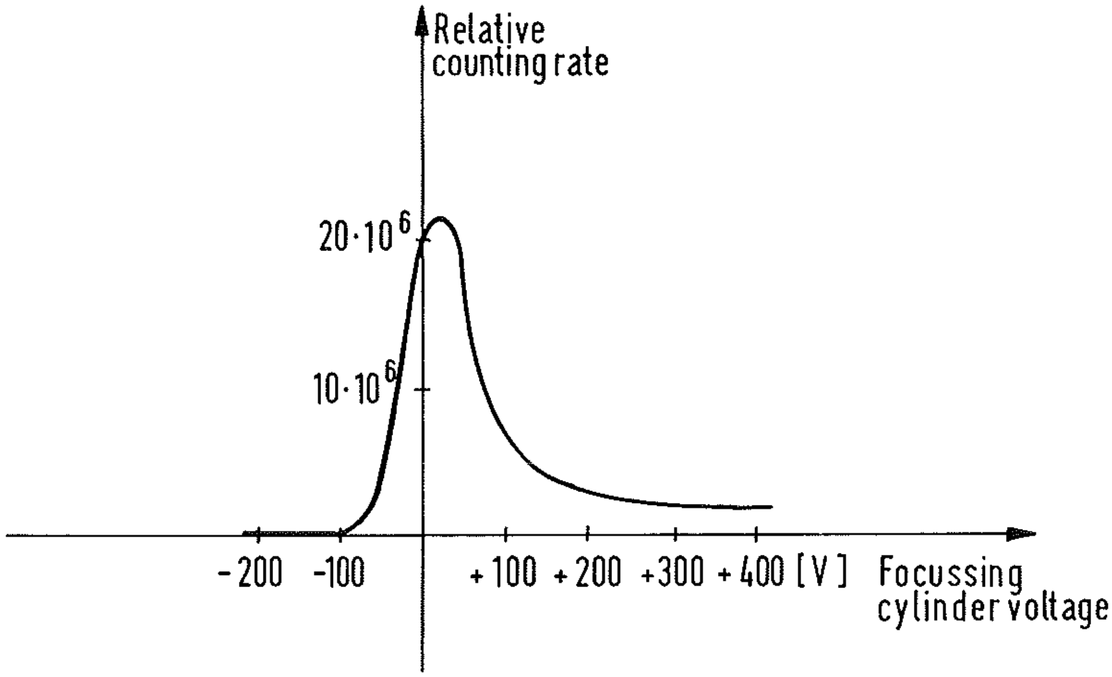


Fig.12 Focussing Effect of the Cylinder Electrode

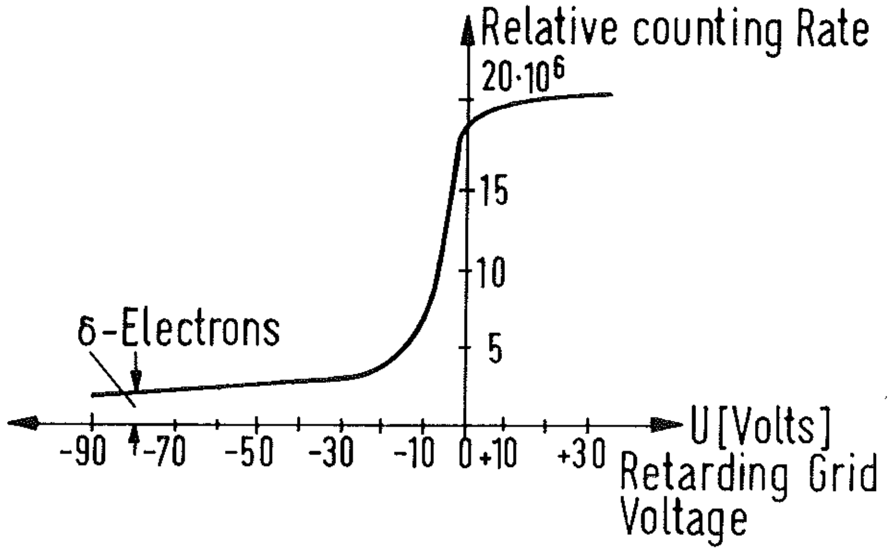


Fig. 13 Decrease of the Counting Rate with increasing Potential Difference between Foil Surface and Grid

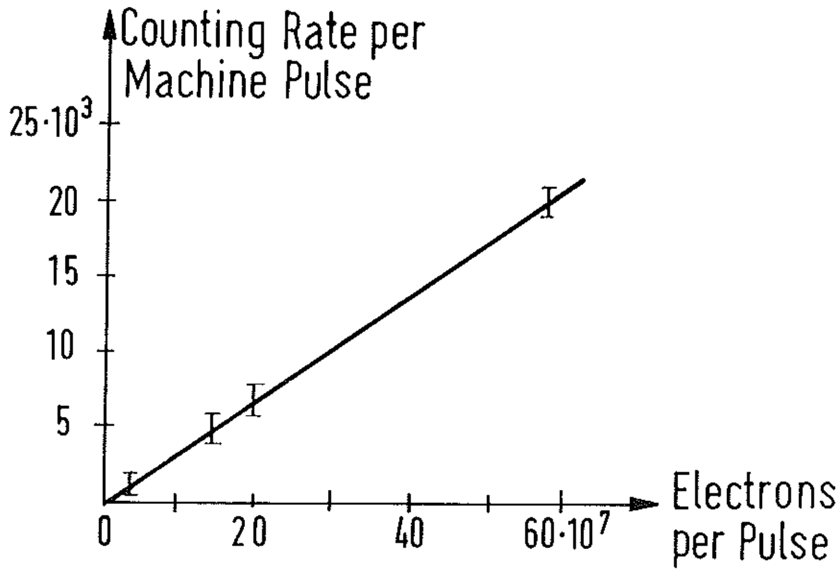


Fig. 14 Range of linear Monitor Response